Measuring Ion Channels on Solid Supported Membranes

Patrick Schulz, Benjamin Dueck, Alexandre Mourot, Lina Hatahet, and Klaus Fendler*
Max Planck Institut für Biophysik, D-60438 Frankfurt/Main, Germany

ABSTRACT Application of solid supported membranes (SSMs) for the functional investigation of ion channels is presented. SSM-based electrophysiology, which has been introduced previously for the investigation of active transport systems, is expanded for the analysis of ion channels. Membranes or liposomes containing ion channels are adsorbed to an SSM and a concentration gradient of a permeant ion is applied. Transient currents representing ion channel transport activity are recorded via capacitive coupling. We demonstrate the application of the technique to liposomes reconstituted with the peptide cation channel gramicidin, vesicles from native tissue containing the nicotinic acetylcholine receptor, and membranes from a recombinant cell line expressing the ionotropic $P2X_2$ receptor. It is shown that stable ion gradients, both inside as well as outside directed, can be applied and currents are recorded with an excellent signal/noise ratio. For the nicotinic acetylcholine receptor and the $P2X_2$ receptor excellent assay quality factors of $Z' = 0.55$ and $Z' = 0.67$, respectively, are obtained. This technique opens up new possibilities in cases where conventional electrophysiology fails like the functional characterization of ion channels from intracellular compartments. It also allows for robust fully automatic assays for drug screening.

INTRODUCTION

Ion channels are important targets for drug discovery because of their physiological significance and their implication in pathogenesis (1). However, robust high throughput screening technologies for ion channels are still scarce and ion channel screening technologies need further innovation, refinement, and optimization (2). Recently, electrophysiological measurements based on solid supported membranes (SSM) have been used for the functional characterization of ion pumps and transporters (3). In this technique, proteoliposomes or membranes (vesicles or fragments) are adsorbed to a SSM and are activated using a rapid substrate concentration jump. Then charge translocation is measured via capacitive coupling of the supporting membrane. This method has the advantage of providing an aqueous environment on both sides of the membrane for the incorporated transport proteins. In addition, adsorption of proteoliposomes or membranes allows a large number of transporters to be immobilized on the electrode in a simple spontaneous process. No complicated incorporation procedures are required.

SSM-based electrophysiology has proven its potential in the field of bacterial transporters (4–8). Physiologically relevant eukaryotic transporters also could be investigated (9,10). Although the latter can be investigated conveniently with conventional electrophysiological methods, SSM-based electrophysiology is attractive because of its robustness and its potential for automation (11,12). This prompted us to investigate the potential of SSM-based electrophysiology for the investigation of ion channels.

SSM-based electrophysiology has been restricted up to now to active transport systems. Investigation of ion channels has been considered to be problematic for various reasons. Adsorbed proteoliposomes and membranes have the disadvantage that no full voltage control over the membrane containing the transporters is attained and that no direct current measurement is possible like in a conventional voltage clamp experiment. This is especially problematic in the investigation of ion channels where transport is usually driven by application of a membrane potential. However, transport through ion channels can also be achieved by application of a gradient of the transported ion. We have, therefore, applied this strategy to measure ion channels in proteoliposomes and membranes adsorbed to a SSM. We show that a stable ion gradient may be established in the system and that this technique allows the functional characterization of ion channels in liposomes as well as in membranes from native tissue and after recombinant expression in a cell line.

MATERIALS AND METHODS

Chemicals

A 1-mM octadecyl-mercaptan (C_{18}-mercaptan; Aldrich, Steinheim, Germany) solution in ethanol was used for the incubation of the gold electrodes. The lipid film forming solutions was diphytanoyl phosphatidylcholin (synthetic; Avanti Polar Lipids, Pelham, AL) and ocadecylamin (60:1, wt/wt, 98%, Riedel-DeHaen AG, Seelze Hannover, Germany). Gramicidin D

Submitted February 12, 2009, and accepted for publication April 13, 2009.

Patrick Schulz and Benjamin Dueck contributed equally to this work.

Benjamin Dueck's present address is London Centre for Nanotechnology and Department of Medicine, University College London, 17- 19 Gordon Street, London WC1H 0AH, UK.

Alexandre Mourot's present address is Department of Molecular and Cell Biology, University of California Berkeley, Berkeley, CA 94720-3200.

*Correspondence: klaus.fendler@mpibp-frankfurt.mpg.de

Editor: Francisco Bezanilla.

0006-3495/09/07/0388/9 $2.00

doi: 10.1016/j.bpj.2009.04.022

from *Bacillus brevis* (Sigma-Aldrich, Taufkirchen, Germany) was dissolved in methanol and stepwise diluted to a 10 μM stock solution.

Liposomes, gramicidin

Liposomes were produced with a LiposoFast-Basic extruder (Avestin, Ottawa, Canada) using 5 mg/mL (w/v) diphytanoyl phosphatidylcholin (Avanti Polar Lipids) in a buffer containing 50 mM HEPES (Tris) pH 7.0 and 10 mM *n*-methylglucamide-chloride (NMGCl). For the preparation of gramicidin liposomes gramicidin from the stock was added to the liposome suspension to a final concentration of 1 μM and incubated for 15 min.

Nicotinic acetylcholine receptor membrane vesicles

Electric organs from small live *Torpedo marmorata* (Biological Station, Roscoff, France) were dissected, frozen in liquid nitrogen, and stored at −80°C. Membranes rich in nicotinic acetylcholine receptor (nAChR) were isolated from frozen electric organs, and further purified using alkali treatment (13). A modified Lowry method (14) was used to determine the protein concentration: 7.4 mg/ml. The specific activity of the membrane preparation (5.5 nmol of acetylcholine (ACh) binding sites/mg of protein) was determined by specific binding of [^{125}I]α-bungarotoxin (New England Nuclear, Boston, MA) using the DEAE filter disk procedure (15). Assuming a molecular mass of 300 kDa for the nAChR, and two ACh binding sites per receptor, the membrane preparation contains ~0.8 mg of nAChR per mg of protein. This preparation consist of predominantly right-side out oriented membrane vesicles with accessible ACh binding sites (16).

Membranes from P2X$_2$ expressing HEK cells

Rat P2X$_2$ (rP2X$_2$) was cloned into pcDNA5/TO using *Bam*HI and *Not*I and the construct was transfected stably in a HEK293 TREx cell line (Invitrogen, Carlsbad, CA) resulting in an inducible cell line, recombinantly expressing rP2X$_2$. Cells were grown in multiple 150 cm^2 culture dishes in DMEM medium, 10% FCS, 1% penicillin/streptomycin, 5 μg/mL blasticidin, and 100 μg/mL hygromycin. When the cells reached a confluence of ~70%–80% they were induced by 1 μg/mL tetracycline and left for protein expression for further 16 hr. Subsequently, cells were collected by centrifugation and disrupted in a Parr Bomb (Parr Instruments Deutschland GmbH, Frankfurt/Main, Germany). The membrane fraction was collected by ultracentrifugation and the plasma membranes were isolated by density gradient centrifugation (3). For long term storage, membranes were flash frozen in resting buffer with 10% glycerol and stored at −80°C. The topology of this membrane preparation is unknown. They could be open membrane fragments or membrane vesicles but for simplicity will be referred to in the following as membrane vesicles.

Protein expression of rP2X$_2$ HEK293 cells was tested by Western blot. Cells were induced for 24 h. Subsequently induced and noninduced cells were lysed in SDS buffer and the lysate was loaded on a 4%–12% bis-Tris gel. After electrophoretic separation proteins were blotted on a PVDF membrane (Invitrogen, Karlsruhe, Germany). The blot was incubated with an anti-P2X$_2$ antibody (APR-003, Alomone, Jerusalem, Israel) (1:400) overnight and with an anti-rabbit-HRP antibody (Amersham Bioscience, Pittsburgh, PA) (1:5000) for 1 h. Chemiluminescent bands were detected using x-ray films. MagicMark XP (Invitrogen) were used for molecular weight markers.

SSM-based electrophysiology

Two different instruments for SSM-based electrophysiology were used: a home-made laboratory SSM set-up (referred to as SSM set-up in the following) and a commercial SURFE^{2}R One instrument (IonGate Biosciences, Frankfurt, Germany). In the SSM set-up the SSM was prepared by linking an alkanethiol (octadecyl mercaptan) monolayer to a gold electrode deposited on a glass support and covering it with a lipid monolayer (Fig. 1). The planar membrane formed has an area of ~0.8 mm^2. The SSM is mounted in a flow-through cuvette with an inner volume of 17 μL. The gold electrode is connected to an amplifier, reference electrode is an Ag/AgCl electrode separated from the solution by a salt bridge. For details of the set-up see Zhou et al. (5) and Pintschovius and Fendler (17).

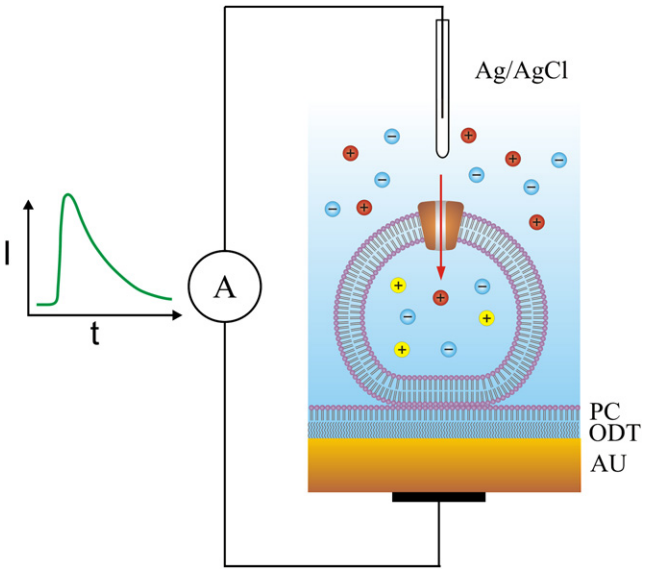

FIGURE 1 Liposomes or membrane vesicles containing a cation channel are adsorbed to the SSM. The SSM consists of an octadecanethiol layer (ODT) covered by a phosphatidylcholine monolayer (PC) on a gold substrate (AU). The liposomes or membrane vesicles are filled with an impermeant cation (yellow) while a permeant cation (red) is rapidly applied to the outside solution. The figure illustrates the principle of capacitive coupling. For clarity, only a single ion channel is shown although liposomes and membrane vesicles typically contain several hundreds of ion channels.

The experiments were carried out at room temperature (22°C). After the formation of the SSM, liposomes, membrane vesicles, or membrane fragments were allowed to adsorb for a period of ~90 min during which capacitance and conductance of the SSM were monitored. After this time, typically stable values of 300–500 nF/cm^2 for the capacitance and 50–100 nS/cm^2 for the conductance were obtained. The putative adsorption geometry of the proteoliposomes and membrane vesicles, respectively, is shown in Fig. 1. Membrane fragments form closed compartments on adsorption that behave like membrane vesicles (3,18). Transient currents through the ion channels were generated by applying a concentration jump of a permeant ion or by activating the channel with an agonist. The solution exchange protocols for the concentration jumps consisted of three or four phases of 0.5- or 1-s duration during which different solutions flowed in each. A pressure of 0.6 bar was applied to drive the solution through the cuvette. A detailed protocol is specified in the figure legends for the different experiments. Data recording and solution exchange were controlled via computer.

For the nAChR stability and all P2X$_2$ measurements the SURFE^{2}R One was operated at a flow rate of 250 μL/sec. nAChR membrane vesicles were allowed to adsorb to the SURFE^{2}R sensors (SSM-area ~7 mm^2) for 1 h. rP2X$_2$ HEK293 membrane vesicles were adsorbed using a centrifugation procedure of 800 × *g* for 45 min. Before mounting the sensor into the SURFE^{2}R One cuvette they were kept in Na^+ free buffer. The solution exchange protocol consisted of four or five phases of 1– 5 s duration each. A detailed protocol is specified in the figure legends. Different substrate or inhibitor concentrations could be applied automatically using the auto sampler of the SURFE^{2}R One instrument.

RESULTS

Gradient driven current through an ion channel

In the constant field approximation, the current through an ion channel is described by the Goldman Hodgkin-Katz equation

$$I = (zF)^2 P \frac{E}{RT} \frac{c_i e^{zEF/RT} - c_o}{e^{zEF/RT} - 1}. \quad (1)$$

Here, E is the membrane potential, and c_o and c_i are the concentrations of the transported ion outside and inside the cell. Ion and channel are characterized by the permeability coefficient P and the valency z. F and R are the Faraday and the gas constants, and T is the temperature. At symmetrical conditions ($c_o = c_i = c$) the Goldman Hodgkin-Katz equation reduces to

$$I = FP \frac{FE}{RT} c. \quad (2)$$

In the absence of a membrane potential ($E = 0$) and if the ion is only present in the intracellular medium ($c_i = c$, $c_o = 0$), the Goldman Hodgkin-Katz Eq. 1 yields

$$I = FPc. \quad (3)$$

This shows that at a given concentration of monovalent positive ions ($z = +1$), a gradient ($c_i = c$, $c_o = 0$) generates the same current as a membrane potential of $E = RT/F =$ 25 mV at symmetrical conditions ($c_o = c_i = c$). This is approximately half of the applied membrane potential in a typical patch clamp experiment and should lead to a measurable charge translocation at the SSM.

Transient currents mediated by the gramicidin channel

Gramicidin is a cation peptide channel from *B. brevis*. Gramicidin incubated liposomes were allowed to adsorb to the SSM as described in materials and methods. The flow protocol for the Na^+ concentration jumps consisted of three flow phases of 0.5 s duration each: first a solution containing the impermeant cation *n*-methylglucamine$^+$ (NMG^+) followed by a permeant cation (Na^+, K^+, Li^+) containing solution and finally the NMG^+ solution again (Fig. 2 *A*). The complete buffer composition is given in the figure legends. The large vertical current spikes at the solution exchange boundaries in Fig. 2 *A* are valve switching artifacts. After a delay of ~30 ms the K^+ containing solution reaches the surface of the SSM and a positive transient current is observed ($t \sim 0.54$ s in Fig. 2 *A*) that represents translocation of positive charge into the liposomes via the gramicidin channels. A transient current in the opposite direction is observed when the K^+ buffer is removed ($t \sim 1.1$ s in Fig. 2 *A*). We will only analyze the valve-on signal because the switching-on behavior of the valve is much better defined.

Control measurements were carried out after addition of gramicidin to the bare SSM, i.e., without liposomes. Gramicidin solution (1 μM) was added to the SSM in the same way as the liposome suspension. These measurements (data not shown) exhibit only negligible transient currents using the solution exchange protocol described above. This shows that gramicidin is not able to establish an ion channel in the hybrid lipid/alkanethiol bilayer of the SSM. Probably insertion or mobility of the gramicidin half channels in the covalently attached alkanthiol layer is not sufficient at the conditions of the experiment.

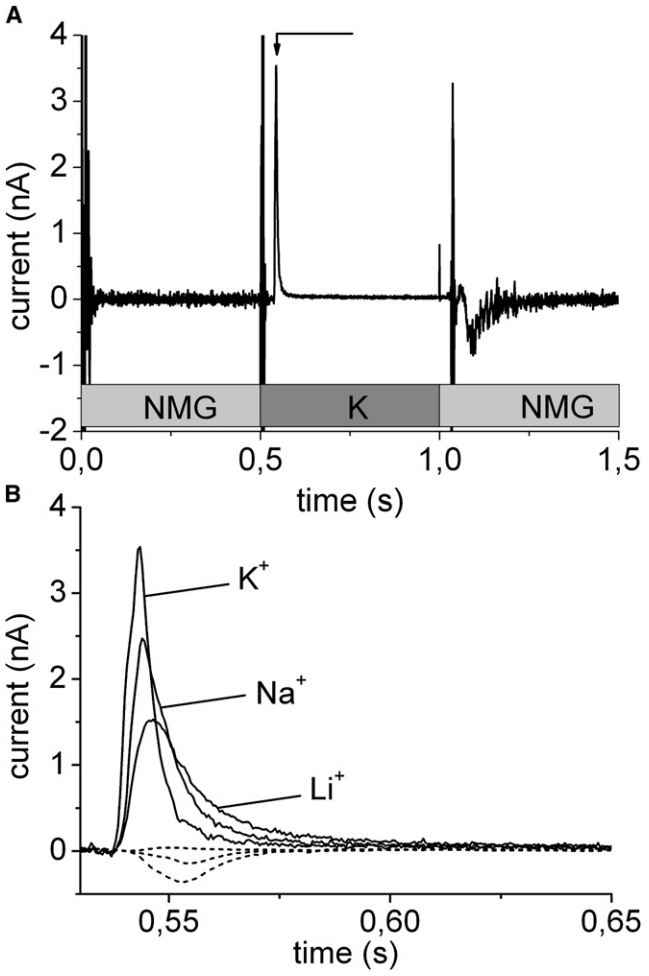

FIGURE 2 Gramicidin channels. (*A*) Solution exchange protocol and transient currents during rapid solution exchange on a SSM with adsorbed liposomes containing gramicidin. The narrow peak currents close to 0.5 and 1 s are valve switching artifacts. Note that the gray boxes indicate timing of the valve driving voltage. Actual valve switching and solution exchange are delayed by up to 50 ms. At $t = 0.5$ s a K^+ containing solution is applied to the SSM. After a short delay time a transient current (*arrow*) indicating translocation of positive charge into the liposome is observed. In addition to a basic buffer of 50 mM Hepes(Tris) pH 7.0 the different solutions contained: 10 mM NMGCl (NMG) or 10 mM KCl (K). (*B*) Expanded view of the transient currents obtained with different cations. For comparison the small negative artifacts obtained in the absence of gramicidin in the liposomes are shown (*dashed lines* in the order of increasing amplitude Li, Na, K). Solution composition as described above except for the permeant cation that was 10 mM KCl (trace K^+), 10 mM NaCl (trace Na^+), and 10 mM LiCl (trace Li^+).

Transient currents could be induced by concentration jumps with Li^+, Na^+, and K^+ (Fig. 2 *B*). The permeability sequence found was $K^+ > Na^+ > Li^+$, which agrees with measurements on planar bilayers (19). As a control, the solution exchange protocol was also applied to the bilayer after addition of liposomes not treated with gramicidin (Fig. 2 *B*). This generated small artifacts of negative (Na^+, K^+) or positive (Li^+) current. These artifacts represent binding of the cations to the SSM (20).

Transient currents mediated by the nAChR

The nAChR is a cation selective ligand gated ion channel expressed in muscle cells and neurons. Subsynaptic fragments prepared from *T. marmorata* electric organ are an abundant source of nAChR (13). We adsorbed these membrane vesicles to a SSM, established a cation gradient across the vesicular membrane, and activated the nAChR conductivity by a rapid concentration jump of 100 μM carbamylcholine (CCh).

The nAChR membrane vesicles were first freeze-thawed and sonicated in a buffer containing the impermeant cation NMG^+ (NMG buffer) to remove other permeant cations from the interior of the vesicles. For the complete buffer composition see Fig. 3 legend. Membrane vesicles were added to the SSM and allowed to adsorb as described before for the gramicidin liposomes. Between experiments the SSM with adsorbed membrane vesicles was kept in the NMG buffer to prevent permeant cations to enter the vesicles and to allow permeant cations introduced in the vesicle during the preceding experiment to be dialyzed out. The flow protocol of a typical experiment is shown in Fig. 3 *A*. First the cation gradient was established by replacing the NMG buffer by a buffer of the same composition but containing 100 mM NaCl instead of NMGCl (Na buffer). At $t \sim 0.45$ s the Na^+ ions reach the SSM creating a solution exchange artifact (Fig. 3 *A*). At $t = 1$ s the Na buffer was replaced by Na buffer containing in addition 100 μM CCh. This generates a rapid positive transient current due to the activation of the nAChR conductivity (Fig. 3 *A*, *arrow*). In the next phase CCh was removed (replacement by Na buffer at $t = 2$ s) and finally the Na buffer was replaced by NMG buffer. CCh removal generated no signal except for a valve switching artifact. Addition of the NMG buffer again created a solution exchange at $t \sim 3.45$ s. In the following, only the rapid transient current at $t \sim 1$ s will be used for the analysis.

The transient currents after addition of CCh are shown in Fig. 4 at an expanded timescale. No signal was obtained if the flow protocol of Fig. 3 *A* was applied to the SSM before the addition of the membrane vesicles. After adsorption of membrane vesicles the same flow protocol yielded a large positive transient current rising and decaying with time constants of 3 ms and 10 ms, respectively (Fig. 4 *A*). The positive current corresponds to the transfer of positive charge in the direction of the electrode that is compatible with Na^+

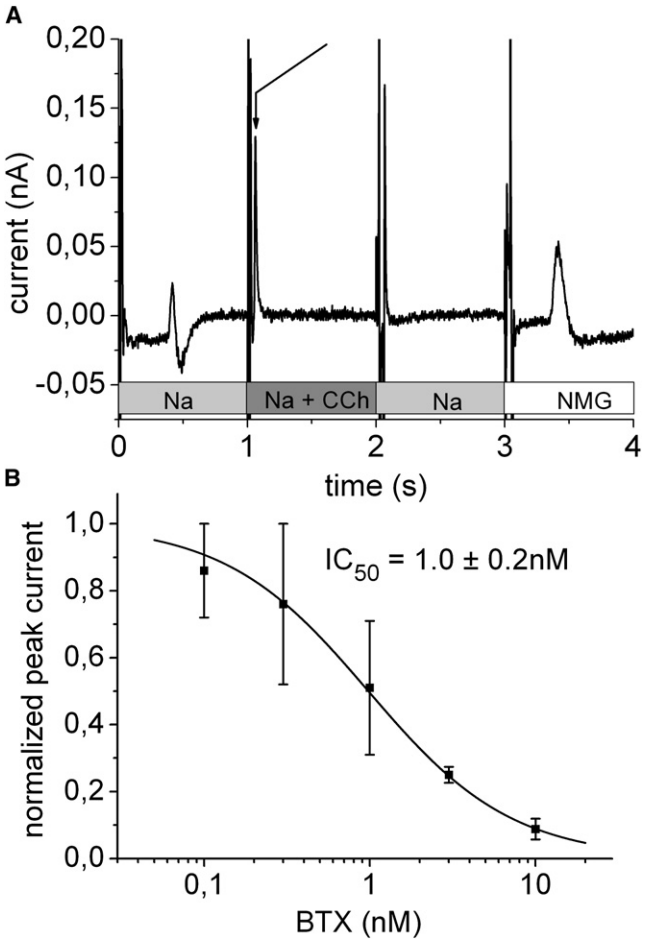

FIGURE 3 nAChR. (*A*) Solution exchange protocol and transient currents during rapid solution exchange on a SSM with adsorbed membrane vesicles containing the nAChR. The positive transient current indicated by the arrow corresponds to the CCh induced Na^+ inflow into the membrane vesicles. Basic buffer in all solutions: 30 mM Tris(HCl) pH 7.5, 3 mM EDTA, 1 mM EGTA. In addition, the different solutions contained: 100 mM NMGCl (NMG), 100 mM NaCl (Na), 100 mM NaCl, and 100 μM CCh (Na + CCh). Before the experiment the membrane vesicles were filled with 100 mM NMGCl. (*B*) Inhibition of the transient currents by the nAChR specific antagonist BTX. Each data point represents three to five independent experiments and error bars (SE) are given. The peak currents for each experiment were normalized to the control value obtained in the absence of BTX. The solid line is a hyperbolic fit to the data.

transport into the liposomes. As a control, CCh addition was tested in the presence of NMG buffer, i.e., no ion gradient was established before the activation of the channel via CCh. This resulted in only a small artifact (Fig. 4 *A*). Finally, the specific nAChR antagonist α-bungarotoxin (BTX) was added to the SSM at a concentration of 100 nM. BTX is a three-finger toxin that associates very slowly and binds almost irreversibly to the acetylcholine binding sites (21). Preincubation of the SSM with BTX for 40 min inhibited the CCh-induced current, yielding only a small artifact as in the previous control.

Transient currents could also be obtained by loading the membrane vesicles with 100 mM NaCl (freeze thaw and

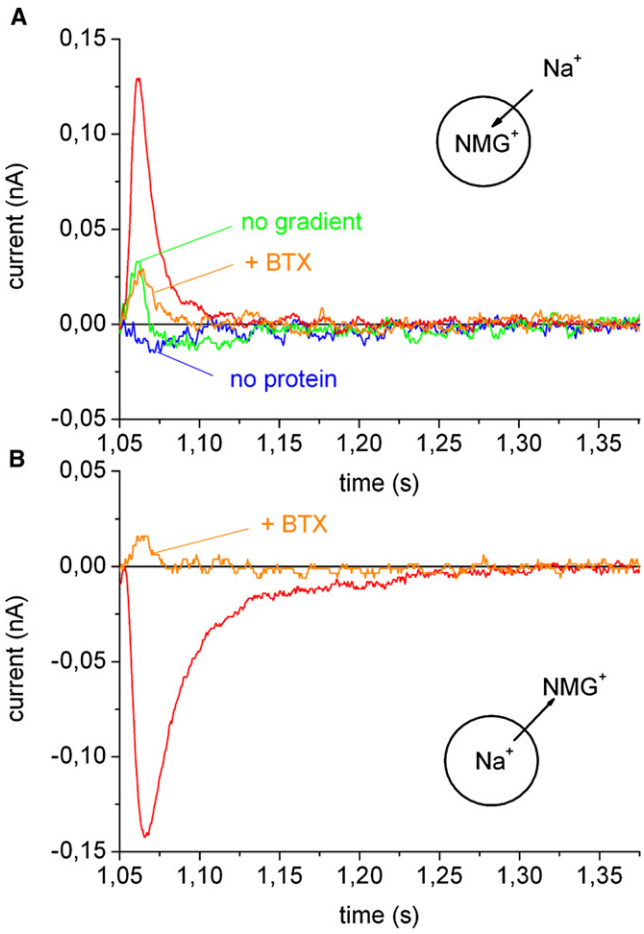

FIGURE 4 nAChR. Na^+ inflow into and Na^+ outflow out of nAChR membrane vesicles. The figure shows an expanded view of the transient currents observed on the SSM. Basic buffer in all solutions: 30 mM Tris(HCl) pH 7.5, 3 mM EDTA, 1 mM EGTA. Additional buffer components are given below. (*A*) Before the experiment the membrane vesicles were filled with 100 mM NMGCl. No label: CCh induced Na^+ inflow. Solution exchange protocol as in Fig. 3 *A*. No protein: control experiment before the membrane vesicles were added. No gradient: Na^+ was exchanged by NMG^+ in all solutions. +BTX: Inhibition with 100 nM BTX. (*B*) Before the experiment the membrane vesicles were filled with 100 mM NaCl. No label: CCh induced Na^+ outflow. Solution exchange protocol as in Fig. 3 *A* but Na^+ was exchanged for NMG^+ and vice versa in all solutions. +BTX: Inhibition with 100 nM BTX.

sonication, see above) and activating the nAChR conductivity by CCh addition in NMG buffer. The transient current obtained by this flow protocol was negative, corresponding to the nAChR mediated outflow of Na^+ from the membrane vesicles (Fig. 4 *B*). The signal had an amplitude comparable to the Na^+ inflow current and decayed with a somewhat larger time constant of 25 ms. BTX (100 nM) inhibited the current proving that it originates from the activity of the nAChR.

The decay time constants of the transient currents is close to the value expected for the time resolution of the system (~20 ms), which is determined by the solution exchange at the SSM surface (22). Therefore, the shape of the signal represents the solution exchange process rather than kinetics of the ion channel. This is not surprising because of the fast turnover of ion channels. The amplitude of the current, on the other hand, represents the transport capacity of the ion channels in the membrane vesicles.

To further characterize the transient currents, a number of control experiments were carried out using solution exchange protocols analogous to Fig. 4 *A*. Variation of the agonist concentration in a range from 1 to 100 μM yielded a dose dependence with an EC_{50} of 13 $\pm$ 1 μM (see Fig. S1 *A* in the Supporting Material). This value agrees well with the CCh concentration for half-maximal $^{22}Na^+$ efflux and influx determined for *Torpedo californica* membranes of ~20 μM (23) or with the range of 10 – 100 μM determined for the *T. marmorata* nAChR from $^{22}Na^+$ efflux (24).

Additional support for the assignment of the transient currents to the activity of the nAChR comes from the concentration dependent BTX inhibition of the Na^+ inflow currents. Inhibition was determined from the peak currents at different BTX concentrations (Fig. 3 *B*). The determined inhibition constant IC_{50} of 1.0 $\pm$ 0.2 nM shows the extremely high affinity of the nAChR for BTX (K_D = 10^{-9} to 10^{-11} for the torpedo nAChR (21)) and unambiguously confirms the assignment of the transient currents.

The nAChR is not very selective among small cations. Nevertheless moderate permeability differences exist. Permeability ratios (relative to Na^+) determined from reversal potential measurements on mouse nAChR give the following series (25) (permeability ratios given in parentheses): NH_4^+ (1.97) > K^+ (1.16) > Na^+ (1) > Li^+ (0.98) > $Tris^+$ (0.36). Comparable values are obtained for the torpedo receptor (26): NH_4^+ (1.83) > Na^+ (1) > $Tris^+$ (0.24). Using the solution exchange protocol of Fig. 3 *A* on the SSM and replacing Na^+ by an alternative cation a somewhat different series is found for the current amplitudes (see Fig. S1*B*): Na^+ (1) > K^+ (0.95) > Li^+ (0.71) > NH_4^+ (0.65) > $Tris^+$ (0.26). The reason for this difference is unclear. It may be related to the fact, that the driving force is the ion gradient rather than the voltage as in the voltage clamp measurements. Permeability ratios are equilibrium properties and not related strictly to the transport capacity of the ion. In addition, the alkaline-treated nAChR preparation used in this study misses the associated protein Rapsyn, which is normally tightly linked to the intracellular vestibule of the nAChR, a region presumably implicated in the ion selectivity (27).

It is important to know how long the cation gradient established by the solution exchange remains stable to yield the necessary driving force for cation transport through the nAChR channel. In the Na^+ inflow experiments of Fig. 3 *A* the transient currents obtained after CCh addition remained stable over many hours. However, if the last phase of the protocol (where the permeant cation Na^+ was replaced by impermeant NMG^+) was omitted, a different behavior was observed. In this case the membrane vesicles were always in NaCl containing buffer (also in between experiments) resulting in a steady decrease of the transient current with

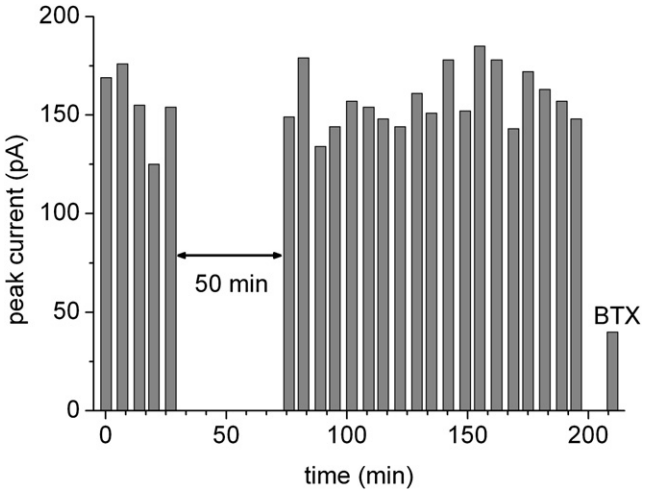

FIGURE 5 nAChR. Stability test of the transient currents. Experimental conditions as in Fig. 3 *A*. Automatic recording of CCh induced currents using a SURFE^{2}R One instrument. At $t = 30$ min recording was stopped for 50 min. After ~3 h nAChR was inhibited with 3 μM BTX.

a time constant of ~20 min. Switching back to the original cation inflow protocol, i.e., NMG buffer incubation in between experiments, restored the signal (see Fig. S2).

To test the robustness of the SSM approach transient currents were repetitively recorded over a period of 3 h on a commercially available SURFE^{2}R One instrument. This allowed a completely automatic execution of the solution exchange protocol every 7 min (Fig. 5). The solution exchange protocol was a slightly modified version of that in Fig. 3 *A*: Na (5 s)/Na$^+$CCh (1 s)/Na (1 s)/NMG (3 s). Stable transient currents varying with a relative standard deviation of ~10% were obtained. The variations are probably due to flow pattern fluctuations at the surface of the SSM. At $t = 30$ min the operation was interrupted for 50 min to test, whether accumulation of ions in the membrane vesicles or charging of the membrane by previous activation affects the signals. This was not the case. After 3 h the nAChR was inhibited by incubation with 3 μM BTX.

Transient currents mediated by the P2X$_2$ receptor

P2X receptors are involved in a number of pathological conditions such as chronic inflammatory and neuropathic pain, brain trauma, and neurodegenerative diseases that makes them important therapeutic targets (28). The rP2X$_2$ receptor, originally cloned from PC12 rat phaeochromocytoma cells (29), is expressed in a variety of neurons in the peripheral and central nervous system, but also pancreas, cochlea, bone, and cardiac muscle (30). The receptor opens in response to extracellular ATP released from neuronal and nonneuronal cells an intrinsic channel for Na^+, K^+, and Ca^{2+}. We used a preparation from a HEK cell line stably expressing rP2X$_2$ receptor to develop an SSM-based assay for this receptor. Expression of the receptor in the prepared membranes was tested by Western blot. The characteristic double band at ~50 and ~60 kD (Fig. 6, *inset*) was obtained corresponding probably to unglycosylated and glycosylated monomers (31). A control whole cell patch clamp measurement yielded ATP-induced inward currents of ~1 nA at −60 mV. The membrane vesicles were adsorbed to an SSM sensor and incubated with tetramethylammonium chloride (TMACl) containing solution, because the P2X receptor has a low permeability for the TMA^+ cation. Using a flow protocol similar to that applied to the nAChR, TMA^+ was replaced by Na^+ to establish a Na^+ ion gradient across the membrane and a transient current response was recorded after addition of ATP in the SURFE^{2}R One instrument (see Fig. 6 legend for complete flow protocol).

In the presence of an inward directed Na^+ gradient (NaCl outside/TMACl inside the membrane vesicles) a positive transient current was observed (Fig. 6) corresponding to

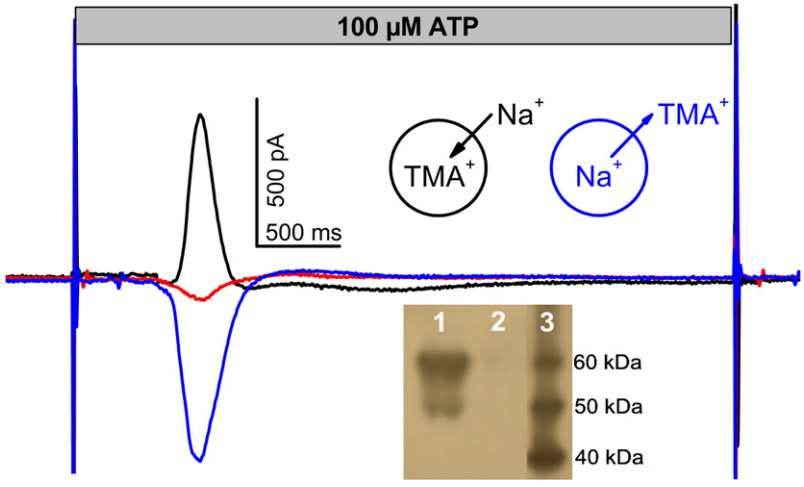

FIGURE 6 P2X$_2$ receptor. Transient current obtained with membrane vesicles from a rP2X$_2$ HEK293 cell line after a 100 μM ATP concentration jump in the presence and absence of Na^+ gradients. *Black line*: Inside directed gradient (Na^+ outside, TMA^+ inside vesicles). *Blue line*: outside directed Na^+ gradient (TMA^+ outside, Na^+ inside vesicles). *Red line*: no gradient (TMA^+ inside and outside vesicles). Experimental conditions: All solutions contained a basic buffer of 50 mM HEPES, 2 mM $MgCl_2$, pH 7.5 (TRIS). A 5-step solution exchange protocol was used consisting of the sequential application of solutions containing basic buffer plus compounds as given below. For the inside directed Na^+ gradient the protocol was (duration given in parentheses): 100 mM TMACl(1 s) − 100 mM NaCl(5 s) − 100 mM NaCl + 100 μM ATP(2 s) (this phase is shown in the figure) − 100 mM NaCl(2 s) − 100 mM TMACl(5 s). To ensure optimal regeneration, the sensors were flushed again for 1 s with 100 mM TMACl 30 s after each measurement and a delay time of 60 s between the measurements was kept. For the outside directed Na^+ gradient TMACl and NaCl were interchanged. In the absence of a Na^+ gradient all solutions contained TMACl. *Inset*: Western blot of rP2X$_2$ HEK293 cells. *Lane 1*: Cell lysate after 24 h tetracycline induction. *Lane 2*: Lysate of noninduced cells. *Lane 3*: Molecular weight marker.

the inflow of Na^+ ions into the vesicles. If no Na^+ gradient was imposed (TMACl outside and inside) only a small ATP solution exchange artifact remained, and if an outward directed Na^+ gradient was present (TMACl outside/NaCl inside) a negative charge displacement was recorded (Fig. 6). Fig. 7*A* shows the amplitude of the transient current at different ATP concentrations. A fit with a Hill function revealed an $EC_{50} = 17 \pm 6$ μM for ATP. This compares well with the reported values of 26 μM (32) in the presence of 1 mM Mg^{2+} or of 16 μM (33) in its absence.

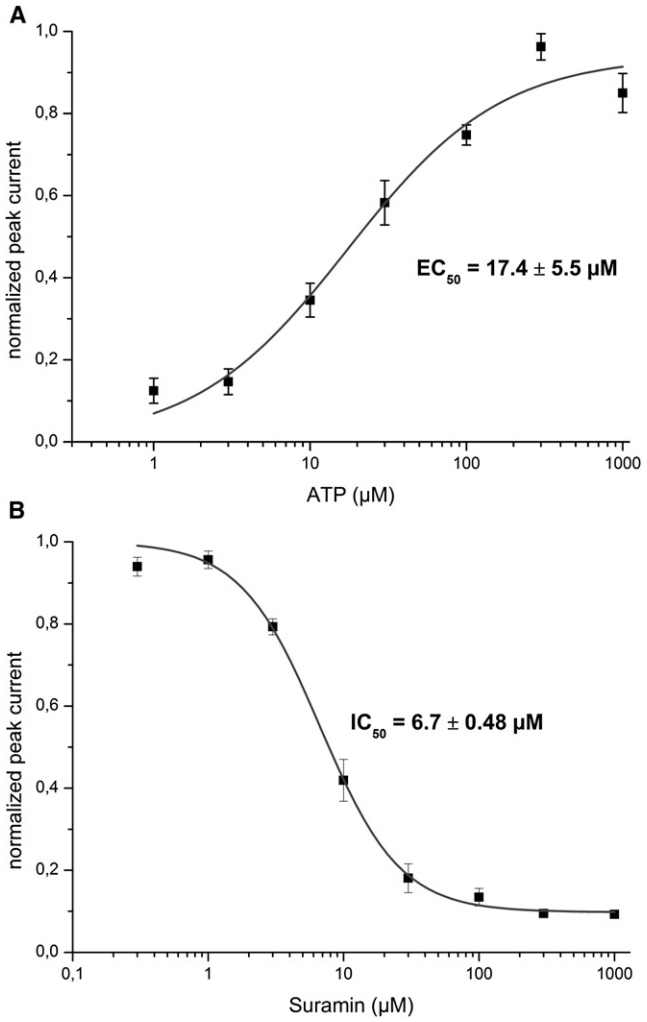

FIGURE 7 $P2X_2$ receptor. (*A*) ATP dependence of transient currents obtained with membrane vesicles from a $rP2X_2$ HEK293 cell line. The plot shows average values (and SE) of four different experiments. Each was normalized to the saturation value of a fit with a Hill function. Subsequently, combined data were fitted with the Hill function, yielding an EC_{50} of 17.4 $\pm$ 5.5 μM and a Hill coefficient of 1.15 $\pm$ 0.44. Experimental conditions as in Fig. 6 but different ATP concentrations (1–1000 mM) were used. (*B*) Inhibition of the $P2X_2$ receptor by suramin. The receptor was activated using a solution exchange protocol as in Fig. 6 with 100 μM ATP in the presence of different concentrations of suramin (0.3–1000 μM) in all buffers. The plot shows mean values (and SE) of six independent experiments. The data were fitted with a Hill function with constant offset yielding an IC_{50} of 6.4 $\pm$ 0.4 μM and a Hill coefficient of 1.55 $\pm$ 0.13.

Suramin and its analogs have been used traditionally as P2X receptor antagonists (34). These compounds exhibit nanomolar to micromolar binding affinities for P2X receptors. The inhibition mechanism of suramin is discussed controversially (35) and the IC_{50} values for inhibition of $P2X_2$ reported in the literature span a wide range from 1 μM to 34 μM (32,33,35–37). In this study, Suramin inhibition was applied as a test for the suitability of our assay for drug characterization. Fig. 7*B* shows the result of the inhibition study with suramin. An $IC_{50} = 6.7 \pm 0.5$ μM was determined that fits well into the range of values determined before, and confirms the assignment of the transient currents to the ATP-induced activation of the $rP2X_2$ ion channel.

DISCUSSION

Ion channels can be characterized by a variety of electrophysiological methods. Conventionally, ion channels of physiological relevance are investigated in mammalian cell lines or oocytes using standard electrophysiology like the patch clamp or the voltage clamp techniques. These measurements are time consuming and require skilled personnel, although recent advances in automated electrophysiology platforms have partially overcome these limitations (38). Planar bilayers (39) and giant vesicles produced by different swelling methods have been used for the investigation of ion channel function (40). They were successfully applied in academic research laboratories but hardly meet the requirements for an industrial drug screening environment. An alternative approach is the reconstitution of ion channels in SSMs. SSMs can be realized on a rugged sensor chip format that readily allows automation and is easy to parallelize. Therefore, great efforts have been undertaken to create SSMs that would allow the measurement of ion channels. Because channels (and also other transport proteins) require an aqueous compartment on both sides of the membrane to accommodate their hydrophilic segments and for binding and release of the charged substrates, membranes have been constructed possessing an aqueous space between the membrane and the solid support, i.e., tethered membranes (41–43). Channel function of biologically relevant ion channels in tethered membranes has been shown in a number of cases like the Clavibacter anion channel (41), the pore-forming toxin α-hemolysin (44), the *Escherichia coli* OmpF porin (45,46), and the pore-forming segment of the acetylcholine receptor (47). It is interesting to note, however, that among all mentioned examples there is no integral eukaryotic ion channel.

We have used an alternative approach by adsorbing proteoliposomes or membrane vesicles containing ion channels to an SSM and recording the transport currents via capacitive coupling. An obvious disadvantage of the technique is that no voltage control over the transport protein is possible in this configuration. Incidentally, metal-supported tethered membranes share the same difficulty of defining the voltage across the membrane containing the transporters (46). The

lack of voltage control is especially problematic for the measurement of ion channels, where conventionally voltage is used as driving force for transport. An ion gradient can be used to drive ions across a channel, however, and at a given ion concentration this corresponds to a driving voltage of up to 25 mV (see Results) in the voltage-driven mode.

This concept was applied to three different systems: 1), a reconstituted liposome system where transport is initiated by the application of a gradient of the transported ion (gramicidin); 2), a native system of membrane vesicles where first an ion gradient is applied and then transport is started by application of the agonist (nAChR); and 3), a recombinant system using stable expression of a ligand gated ion channel in a mammalian cell line ($P2X_2$ receptor). In all cases transient currents could be recorded that reflect the known properties of these ion channels. Control measurements confirmed the assignment of the transient currents to the channel activity of the respective proteins. This is shown unambiguously by the high-affinity BTX inhibition of the nAChR and the specific inhibition of the $P2X_2$ receptor by suramin. The recombinant approach, a routine task in modern molecular biology, opens up SSM-based electrophysiology for the functional characterization of arbitrary ion channels in a host cell line.

SSM-based electrophysiology measures macroscopic channel currents. This makes it well suited for the determination of ion specificity and for pharmacological characterization whereas single channel properties are out of the scope of the technique. We have chosen two ligand gated ion channels, nAChR and $P2X_2$, for good reasons. Because of the lack of voltage control on the SSM, voltage gated ion channels, especially if they are of the rapidly inactivating type, may be problematic.

SSM-based electrophysiology is a robust technique that allows recording of ion channel currents over many hours using the same sensor (Fig. 6). The suitability of an assay technique in an industrial screening environment is usually evaluated on the basis of a Z' factor (48) $Z' = 1 - 3(\sigma_p + \sigma_n)/(\mu_p - \mu_n)$ with the mean values, μ_p and μ_n, and the standard deviations, σ_p and σ_n, of the positive control and the negative control, respectively. For the nAChR the positive and negative controls are the currents in the absence and presence of the inhibitor BTX and may be determined from Fig. 6 yielding $Z' = 0.55$. For the $P2X_2$ receptor the corresponding parameters are determined in the absence and presence of a Na^+ gradient and result in $Z' = 0.67$. These results support the good quality of the SSM-based technology. Note that assays with $Z' > 0.5$ are generally considered as excellent.

This study represents what we believe is the first measurement of the transport activity of integral eukaryotic ion channels on an SSM. Convenient and robust functional assays with an excellent quality are obtained. It is shown that SSM-based electrophysiology works for ion channels in liposomes and native tissue as well as with channels recombinantly overexpressed in a cell line. Because the technique can be automated readily and has been adapted already to an industry standard 96-well plate format (18) it has great potential for application in high throughput drug discovery. In addition, the method opens up new possibilities when the use of conventional electrophysiology fails as in the case of ion channels from intracellular compartments.

SUPPORTING MATERIAL

Two figures are available at http://www.biophysj.org/biophysj/supplemental/S0006-3495(09)00848-0.

We thank Maurice Goeldner for generously sharing the nAChR membrane preparation prepared in his laboratory, Jürgen Rettinger and Günther Schmalzing for the $rP2X_2$ clone and helpful discussions, Ulrich Terpitz for the test patch clamp measurements with rP2X2 HEK293 cells, Ernst Bamberg for his continuing interest and support, Bela Kelety and Henning Vollert for helpful discussions, and Martin Stein for technical assistance.

REFERENCES

1. Hubner, C. A., and T. J. Jentsch. 2002. Ion channel diseases. *Hum. Mol. Genet.* 11:2435–2445.
2. Zheng, W., R. H. Spencer, and L. Kiss. 2004. High throughput assay technologies for ion channel drug discovery. *Assay Drug Dev. Technol.* 2:543–552.
3. Schulz, P., J. J. Garcia-Celma, and K. Fendler. 2008. SSM-based electrophysiology. *Methods.* 46:97–103.
4. Burzik, C., G. Kaim, P. Dimroth, E. Bamberg, and K. Fendler. 2003. Charge displacements during ATP-hydrolysis and synthesis of the Na^+-transporting FoF1-ATPase of *Ilyobacter tartaricus*. *Biophys. J.* 85:2044–2054.
5. Zhou, A., A. Wozniak, K. Meyer-Lipp, M. Nietschke, H. Jung, et al. 2004. Charge translocation during cosubstrate binding in the Na^+/proline transporter of *E. coli*. *J. Membr. Biol.* 343:931–942.
6. Meyer-Lipp, K., C. Ganea, T. Pourcher, G. Leblanc, and K. Fendler. 2004. Sugar binding induced charge translocation in the melibiose permease from *Escherichia coli*. *Biochemistry.* 43:12606–12613.
7. Zuber, D., R. Krause, M. Venturi, E. Padan, E. Bamberg, et al. 2005. Kinetics of charge translocation in the passive downhill uptake mode of the Na^+/H^+ antiporter NhaA of *Escherichia coli*. *Biochim. Biophys. Acta.* 1709:240–250.
8. Raunser, S., M. Appel, C. Ganea, U. Geldmacher-Kaufer, K. Fendler, et al. 2006. Structure and function of prokaryotic glutamate transporters from *Escherichia coli* and *Pyrococcus horikoshii*. *Biochemistry.* 45:12796–12805.
9. Pintschovius, J., K. Fendler, and E. Bamberg. 1999. Charge translocation by the Na^+/K^+-ATPase investigated on solid supported membranes: cytoplasmic cation binding and release. *Biophys. J.* 76:827–836.
10. Tadini-Buoninsegni, F., G. Bartolommei, M. R. Moncelli, R. Guidelli, and G. Inesi. 2006. Pre-steady state electrogenic events of Ca^{2+}/H^+ exchange and transport by the Ca^{2+}-ATPase. *J. Biol. Chem.* 281: 37720–37727.
11. Kelety, B., K. Diekert, J. Tobien, N. Watzke, W. Dörner, et al. 2006. Transporter assays using solid supported membranes: a novel screening platform for drug discovery. *Assay Drug Dev. Technol.* 4:575–582.
12. Geibel, S., N. Flores-Herr, T. Licher, and H. Vollert. 2006. Establishment of cell-free electrophysiology for ion transporters: application for pharmacological profiling. *J. Biomol. Screen.* 11:262–268.
13. Neubig, R. R., E. K. Krodel, N. D. Boyd, and J. B. Cohen. 1979. Acetylcholine and local anesthetic binding to Torpedo nicotinic postsynaptic membranes after removal of nonreceptor peptides. *Proc. Natl. Acad. Sci. USA.* 76:690–694.

14. Peterson, G. L. 1977. A simplification of the protein assay method of Lowry, et al. which is more generally applicable. *Anal. Biochem.* 83:346–356.

15. Schmidt, J., and M. A. Raftery. 1973. A simple assay for the study of solubilized acetylcholine receptors. *Anal. Biochem.* 52:349–354.

16. Hartig, P. R., and M. A. Raftery. 1979. Preparation of right-side-out, acetylcholine receptor enriched intact vesicles from *Torpedo californica* electroplaque membranes. *Biochemistry.* 18:1146–1150.

17. Pintschovius, J., and K. Fendler. 1999. Charge translocation by the Na^+/K^+-ATPase investigated on solid supported membranes: rapid solution exchange with a new technique. *Biophys. J.* 76:814–826.

18. Krause, R., N. Watzke, B. Kelety, W. Dorner, and K. Fendler. 2009. An automatic electrophysiological assay for the neuronal glutamate transporter mEAAC1. *J. Neurosci. Methods.* 177:131–141.

19. Bamberg, E., K. Noda, E. Gross, and P. Lauger. 1976. Single-channel parameters of gramicidin A, B, and C. *Biochim. Biophys. Acta.* 419: 223–228.

20. Garcia-Celma, J., L. Hatahet, W. Kunz, and K. Fendler. 2007. Specific anion and cation binding to lipid membranes investigated on a solid supported membrane. *Langmuir.* 23:10074–10080.

21. Nirthanan, S., and M. C. E. Gwee. 2004. Three-finger alpha-neurotoxins and the nicotinic acetylcholine receptor, forty years on. *J. Pharmacol. Sci.* 94:1–17.

22. Garcia-Celma, J. J., B. Dueck, M. Stein, M. Schlueter, K. Meyer-Lipp, et al. 2008. Rapid activation of the melibiose permease MelB immobilized on a solid-supported membrane. *Langmuir.* 24:8119–8126.

23. Walker, J. W., R. J. Lukas, and M. G. McNamee. 1981. Effects of thiogroup modifications on the ion permeability control and ligand binding properties of *Torpedo californica* acetylcholine receptor. *Biochemistry.* 20:2191–2199.

24. Hazelbauer, G. L., and J. P. Changeux. 1974. Reconstitution of a chemically excitable membrane. *Proc. Natl. Acad. Sci. USA.* 71:1479–1483.

25. Cohen, B. N., C. Labarca, N. Davidson, and H. A. Lester. 1992. Mutations in M2 alter the selectivity of the mouse nicotinic acetylcholine receptor for organic and alkali metal cations. *J. Gen. Physiol.* 100:373–400.

26. Wang, F., and K. Imoto. 1992. Pore size and negative charge as structural determinants of permeability in the Torpedo nicotinic acetylcholine receptor channel. *Proc. Biol. Sci.* 250:11–17.

27. Unwin, N. 2005. Refined structure of the nicotinic acetylcholine receptor at 4 angstrom resolution. *J. Mol. Biol.* 346:967–989.

28. Gever, J. R., D. A. Cockayne, M. P. Dillon, G. Burnstock, and A. Ford. 2006. Pharmacology of P2X channels. *Pflugers Arch.* 452:513–537.

29. Brake, A. J., M. J. Wagenbach, and D. Julius. 1994. New structural motif for ligand-gated ion channels defined by an ionotropic ATP receptor. *Nature.* 371:519–523.

30. North, R. A. 2002. Molecular physiology of P2X receptors. *Physiol. Rev.* 82:1013–1067.

31. Suzuki-Kerr, H., S. Vlajkovic, P. J. Donaldson, and J. Lim. 2008. Molecular identification and localization of P2X receptors in the rat lens. *Exp. Eye Res.* 86:844–855.

32. King, B. F., S. S. Wildman, L. E. Ziganshina, J. Pintor, and G. Burnstock. 1997. Effects of extracellular pH on agonism and antagonism at a recombinant P2X2 receptor. *Br. J. Pharmacol.* 121:1445–1453.

33. Wildman, S. S., B. F. King, and G. Burnstock. 1998. Zn^{2+} modulation of ATP-responses at recombinant P2X2 receptors and its dependence on extracellular pH. *Br. J. Pharmacol.* 123:1214–1220.

34. Bultmann, R., H. Wittenburg, B. Pause, G. Kurz, P. Nickel, et al. 1996. P2-purinoceptor antagonists: III. Blockade of P2-purinoceptor subtypes and ecto-nucleotidases by compounds related to suramin. *Naunyn Schmiedebergs Arch. Pharmacol.* 354:498–504.

35. Trujillo, C. A., A. A. Nery, A. H. Martins, P. Majumder, F. A. Gonzalez, et al. 2006. Inhibition mechanism of the recombinant rat P2X(2) receptor in glial cells by suramin and TNP-ATP. *Biochemistry.* 45:224–233.

36. Bianchi, B. R., K. J. Lynch, E. Touma, W. Niforatos, E. C. Burgard, et al. 1999. Pharmacological characterization of recombinant human and rat P2X receptor subtypes. *Eur. J. Pharmacol.* 376:127–138.

37. Evans, R. J., C. Lewis, G. Buell, S. Valera, R. A. North, et al. 1995. Pharmacological characterization of heterologously expressed ATP-gated cation channels (P2x purinoceptors). *Mol. Pharmacol.* 48:178–183.

38. Castle, N., D. Printzenhoff, S. Zellmer, B. Antonio, A. Wickenden, et al. 2009. Sodium channel inhibitor drug discovery using automated high throughput electrophysiology platforms. *Comb. Chem. High Throughput Screen.* 12:107–122.

39. Morera, F. J., G. Vargas, C. Gonzalez, E. Rosenmann, and R. Latorre. 2007. Ion-channel reconstitution. *Methods Mol. Biol.* 400:571–585.

40. Keller, B. U., R. Hedrich, W. L. Vaz, and M. Criado. 1988. Single channel recordings of reconstituted ion channel proteins: an improved technique. *Pflugers Arch.* 411:94–100.

41. Michalke, A., T. Schurholz, H. J. Galla, and C. Steinem. 2001. Membrane activity of an anion channel from *Clavibacter michiganense* ssp. *nebraskense*. *Langmuir.* 17:2251–2257.

42. Friedrich, M. G., M. A. Plum, M. G. Santonicola, V. U. Kirste, W. Knoll, et al. 2008. In situ monitoring of the catalytic activity of cytochrome *c* oxidase in a biomimetic architecture. *Biophys. J.* 95: 1500–1510.

43. Purrucker, O., A. Fortig, R. Jordan, and M. Tanaka. 2004. Supported membranes with well-defined polymer tethers-incorporation of cell receptors. *ChemPhysChem.* 5:327–335.

44. Glazier, S. A., D. J. Vanderah, A. L. Plant, H. Bayley, G. Valincius, et al. 2000. Reconstitution of the pore-forming toxin alpha-hemolysin in phospholipid/18-octadecyl-1-thiahexa(ethylene oxide) and phospholipid/n-octadecanethiol supported bilayer membranes. *Langmuir.* 16:10428–10435.

45. Gritsch, S., P. Nollert, F. Jahnig, and E. Sackmann. 1998. Impedance spectroscopy of porin and gramicidin pores reconstituted into supported lipid bilayers on indium-tin-oxide electrodes. *Langmuir.* 14:3118–3125.

46. Moncelli, M. R., L. Becucci, and S. M. Schiller. 2004. Tethered bilayer lipid membranes self-assembled on mercury electrodes. *Bioelectrochemistry.* 63:161–167.

47. Vockenroth, I. K., P. P. Atanasova, J. R. Long, A. T. A. Jenkins, W. Knoll, et al. 2007. Functional incorporation of the pore forming segment of AChR M2 into tethered bilayer lipid membranes. *Biochim. Biophys. Acta.* 1768:1114–1120.

48. Zhang, J. H., T. D. Chung, and K. R. Oldenburg. 1999. A simple statistical parameter for use in evaluation and validation of high throughput screening assays. *J. Biomol. Screen.* 4:67–73.